Synthesis of Poly(vinyl pyridine)–Silica Nanocomposites Using Perhydropolysilazane

Reiko Saito, Tadakuni Tobe

Department of Organic and Polymeric Materials, Tokyo Institute of Technology, 2-12, Ookayama, Meguro-ku, Tokyo, 152-8552, Japan

Received 23 September 2003; accepted 27 January 2004
DOI 10.1002/app.20544
Published online in Wiley InterScience (www.interscience.wiley.com).

ABSTRACT: Poly(2-vinyl pyridine)/silica and poly(4-vinyl pyridine)/silica nanocomposites were synthesized by casting of blend solutions of perhydropolysilazane and poly(2-vinyl pyridine-*co*-2-hydroxyethyl methacrylate) and poly(4-vinyl pyridine-*co*-2-hydroxyethyl methacrylate) random copolymers, respectively, and calcination of dried films at 100°C under steam. The structures of the separated phases and the thermal properties of the composites were investigated by transmission electron microscopy (TEM), DSC, and TGA. © 2004 Wiley Periodicals, Inc. J Appl Polym Sci 93: 749–757, 2004

Key words: nanocomposites; silicas; phase separation; thermal properties; poly(vinyl pyridine) PVC

INTRODUCTION

It is well known that silica is a useful additive to improve the properties of organic polymes, such as thermal stability, mechanical strength, transparency, and insulation.[1–6] The sol–gel method is one of the useful and convenient methods to prepare organic/silica hybrid composites. The major advantages of the sol–gel method are lower reaction temperature than decomposition temperature of organic polymer and high applicability to many kinds of organic polymers.[7–13] On the other hand, the control of inner structure of the composites prepared by the sol–gel method is insufficient.

To design highly functional organic/silica composites, microscopically strict control of inner structure of the composites is strongly required. It is well known that block and graft copolymers with incompatible sequences form microphase separation in nanoscale.[14,15] When molecular weight distribution of the copolymers is narrow and the content of each sequence is unity, the microphase separation is well ordered. The ordered microphase separation of the copolymers is a good template of organic/silica composites. Based on this consideration, the block copolymers with polyhedral oligomeric silsesquioxane (POSS) sequence as silica sequence have been synthesized and their microphase separation was investigated.[16,17] However, it was impossible to obtain organic/silica composites with high POSS content, because the solubility of POSS is low in many organic solvents, which are good solvents for organic polymers.

Perhydropolysilazane (PHPS), which is well known as a preceramic material of silica, is highly soluble in many organic solvents, such as benzene, toluene, xylene, pyridine, tetrahydrofurane, etc., and is highly multireactive with hydroxyl group. Thus, it is possible to graft PHPS onto organic polymers that contain hydroxyl group. When the organic polymer is soluble in the organic solvent in which PHPS is dissolved, the graft copolymer will be soluble to the organic solvent. By blending PHPS and the organic polymer with hydroxyl group in the organic solvent and casting the blend solution, the organic/PHPS film with organic polymer and PHPS microdomains will be obtained.

Another interesting feature of PHPS is its mild calcination conditions: the calcination temperature lies between room temperature to 100°C, no catalyst, except for steam, is required. The organic polymer in the composites will not be decomposed in this temperature range. Additionally, the PHPS microdomains of the organic/PHPS film will be converted to the silica microdomain without changing the shape and size of the microdomains. Therefore, the organic/silica nanocomposite will be conveniently formed from organic polymer by blending with PHPS, casting the blend solution and calcination of the organic/PHPS film. The synthesis of organic/silica nanocomposites with PHPS is schematically shown in Figure 1. Based on this consideration, copolymer/silica nanocomposites were successfully obtained by blending PHPS with poly(methyl methacrylate-*co*-2-hydroxyethyl methac-

Correspondence to: R. Saito (rsaito@polymer.titech.ac.jp).
Contract grant sponsor: Tokuyama Science Foundation.

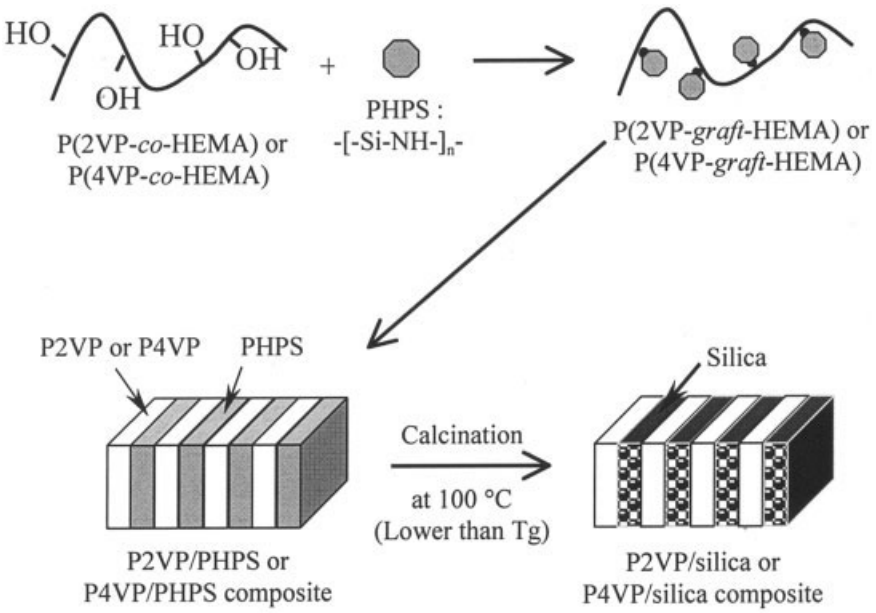

Figure 1 Synthetic scheme of organic/silica nanocomposites with perhydropolysilazane, PHPS.

rylate)[18] or poly(methyl methacrylate)-*block*-poly(methyl methacrylate-*co*-2-hydroxyethyl methacrylate).[19,20]

From our previous investigations,[18–20] the following important points for the synthesis of the composites with PHPS were established. (1) Polymer concentration in the blend solutions should be lower than 1 wt %. (2) Content of hydroxyl groups in the polymer should be lower than 33 mol %. As described above, PHPS is a multireactive material with hydroxyl group. When the polymer concentration and hydroxyl content of the polymer were high, PHPS act as a crosslinker, and the blend solution was gelled. The choice of solvent for blending is also important. Previously, benzene and THF were used, which are poor solvents for hydroxyl groups and good solvents for the rest of organic polymer. In such a selective solvent, the hydroxyl group is segregated, so gelation should be enhanced. As well as decreases of the content of hydroxyl group in polymer and polymer concentration, nonselective solvent will hinder the macrogelation of the blend solution. Better control over the microphase separation of the nanocomposites is expected for the nonselective solvent.

The purpose of this work is to investigate the solvent effect on the gelation behavior of the blend solutions and the nanostructure of the composites. Thus, pyridine, dimethylsulfoxide, (DMSO), which are nonselective solvents, and tetrahydrofuran (THF) were chosen. Poly(2-vinyl pyridine-*co*-2-hydroxyethyl methacrylate) [P(2VP-*co*-HEMA)] and poly(4-vinyl pyridine-*co*-2-hydroxyethyl methacrylate) [P(4VP-*co*-HEMA)] were synthesized by radical copolymerization with α,α'-azobis-isobutylonitrile (AIBN) and were employed as the organic copolymers. P2VP and P4VP can be converted to conducting polymers by the neutralization with HCl and by the quaternization with methyl iodide, respectively.[21,22] P2VP/silica and P4VP/silica nanocomposites will be obtained with P(2VP-*co*-HEMA) and P(4VP-*co*-HEMA), respectively. P2VP/silica and P4VP/silica nanocomposites have been synthesized by formation of silica nano-particles with P2VP and P4VP, respectively.[23–25] Because silica nanoparticles were used, the morphologies of the silica domain within the composites was spherical. On the other hand, when PHPS is used, silica domain with nonspherical morphologies is expected. Thus, P2VP/silica and P4VP/silica nanocomposites with many types of silica domains were also targeted in this work.

Inner structures of the composites were observed by transmission electron microscopy (TEM). Glass transition temperatures (T_g) and thermal stabilities of the composites, were measured by differential scanning calorimetry (DSC) and thermalgravimetric analysis (TGA).

EXPERIMENTAL

Materials

2-Vinyl pyridine (2VP) (Tokyo Kasei Organic Chemicals Co. Ltd., 97%), 4-vinyl pyridine (4VP) (Tokyo Kasei Organic Chemicals Co. Ltd., 97%), and 2-hydroxyethyl methacrylate (HEMA) (Kanto Chemical Co. Inc., 95%) were purified by distillation under vacuum.

Benzene (Kanto Chemical Co. Inc., 99%), 1-propanol (Kanto Chemical Co. Inc., 99%), *n*-hexane (Kanto Chemical Co. Inc., 95%), α,α'-azobisisobutyronitrile (AIBN) (Kanto Chemical Co. Inc., 97%), perhydropol-

ysilazane (PHPS)/xylene solution (NN-110, Clariant Japan Co., PHPS concentration = 20 wt %, M_w of PHPS = 700) were used without purification.

Cyclohexane (Kanto Chemical Co. Inc., 99%), and tetrahydrofurane (THF) (Kanto Chemical Co. Inc., 97%) were dried using sodium metal and distilled under vacuum. Pyridine (Kanto Chemical Co. Inc., 99%) and dimethyl sulfoxide (DMSO) (Kanto Chemical Co. Inc., 99%) were dried using calcium hydride and then distilled under vacuum.

Synthesis of poly(2-vinyl pyridine-*co*-2-hydroxyethyl methacrylate) [P(2VP-*co*-HEMA)] and poly(4-vinyl pyridine-*co*-2-hydroxyethyl methacrylate) [P(4VP-*co*-HEMA)]: P(2VP-*co*-HEMA) and P(4VP-*co*-HEMA) were synthesized by radical polymerization with AIBN in chloroform at 70°C under nitrogen atmosphere. The synthetic procedure for P(2VP-*co*-HEMA) is typically as follows: 2VP (7.0 mL), HEMA (1.0 mL), AIBN (0.142 g) were dissolved in benzene (20 mL) and 1-propanol (10 mL) in a glass reactor. The air in the reactor was evacuated at room temperature. Then, the reactor was sealed under vacuum and heated at 70°C for 10 h. After the heating, the reactor was cooled to room temperature. To precipitate polymer, the solution in the reactor was poured into excess *n*-hexane (100 mL). The precipitated polymer was collected, purified twice by reprecipitation method, with methanol (20 mL) and water (100 mL) as a good solvent and a precipitant, respectively, and dried under vacuum.

Characterization

Molecular weight (M_v) of all polymers was determined by viscometric measurements in a ethanol–water mixture (weight fraction of water: 8.0%) at 25°C using the following equations:[26] $[\eta] = 1.22 \times 10^{-2} \times M^{0.73}$ and $[\eta] = 1.20 \times 10^{-2} \times M^{0.73}$ for P(2VP-*co*-HEMA) and P(4VP-*co*-HEMA), respectively. The HEMA content, 15%, was ignored ass a first apporoximation. The HEMA content was measured using ^{1}H-NMR (JEOL, GLX-500, 500 MHz) with deutererated diemthyl sulfoxide as a solvent.

Preparation and calcination of blend films of polymer and PHPS

One weight percent of polymer solution and a certain amount of NN-110 were mixed under nitrogen atmosphere. The mixture was stirred at 20°C for 24 h. After sampling a small amount of this mixture for the investigation of graft formation, the mixture was cast on a Teflon dish and gradually dried under dried nitrogen atmosphere. Dried films were heated at 100°C for 4 h under steam.

Characterization of graft copolymer

Graft copolymer in the sampled mixture was recovered by precipitation into *n*-hexane and dried. The PHPS content of the graft copolymer was measured with a Fourrier-transform infrared spectrometer (Jasco, FT/IR-410, resolution: 1 cm^{-1}) by using absorption at 835 and 1730 cm^{-1} due to the Si—N stretching in PHPS and the carbonyl group in methacrylates, respectively.

TABLE I
Characteristics of Poly(2-vinyl pyridine-*co*-2-hydroxyethyl methacrylate) [P(2VP-*co*-HEMA)], and Poly(4-vinly pyridine-*co*-2-hydroxyethyl methacrylate) [P(4VP-*co*-HEMA)]

Code	$M\nu$[a]	HEMA content[b] (mol %)
P(2VP-*co*-HEMA)	3.58×10^4	15.0
P(4VP-*co*-HEMA)	4.34×10^4	16.0

[a] Viscometric molecular weight.
[b] Determined by ^{1}H-NMR.

Transmission electron microscopy

Ultrathin specimens of the composites before and after calcination were microtomed with cryomicrotome (Reichert-Nissei, Ultracut-N) using a diamond blade. The internal morphology of the specimens was observed with a transmission electron microscope (JEOL, JEM-200CX) with 80 kV without staining.

Thermogravimetric analysis (TGA)

TGA was performed with a SEIKO EXSTAR-600TG/DTA6300 thermogravimeter up to 600°C at a heating rate of 10 K min^{-1}.

RESULTS AND DISUCSSION

Synthesis of random copolymers

P(2VP-*co*-HEMA) and P(4VP-*co*-HEMA) were synthesized by free radical polymerization with AIBN. The viscosity molecular weight and HEMA contents are listed in Table I. HEMA contents were 15.0 and 16.0 mol % for P(2VP-*co*-HEMA) and P(4VP-*co*-HEMA), respectively. PMMA/silica composites with ordered nanostructures were previously obtained with a HEMA content of 14.5 mol %. Thus, P2VP/silica and P4VP/silica composites with ordered nanostructure were expected in this work.

As well as HEMA content, the localization of HEMA in the copolymers may be important in nanocomposite formation. Monomer reactivity ratios r_1 and r_2 were calculated using Q and e values of HEMA, 2VP, and 4VP, to be (0.535, 1.145) and (0.727, 1.092) where monomer 1 = HEMA and monomer 2 = 2VP, or 4VP, respectively. This indicates that HEMA groups are randomly distributed in P(2VP-*co*-HEMA)

TABLE II
Conditions and Results of Synthesis of Composites

Code	Polymer	Solvent	[PHPS]/[HEMA] (mol/mol)[a]	G_{PHPS} (mol %)[b]	Weight faction of silica (wt %)[c]		
					Grafted	Ungrafted	Overall
2VP-0.5P	P(2VP-*co*-HEMA)	Pyridine	0.5	24.9	9.3	28.0	37.3
2VP-1.0P	P(2VP-*co*-HEMA)	Pyridine	1.0	50.5	27.4	26.9	54.3
2VP-1.5P	P(2VP-*co*-HEMA)	Pyridine	1.5	50.2	32.2	31.9	64.1
2VP-0.5T	P(2VP-*co*-HEMA)	THF	0.5	100.0	37.3	0.0	37.3
2VP-1.0T	P(2VP-*co*-HEMA)	THF	1.0	100.0	54.3	0.0	54.3
2VP-1.5T	P(2VP-*co*-HEMA)	THF	1.5	100.0	64.1	0.0	64.1
4VP-0.5P	P(4VP-*co*-HEMA)	Pyridine	0.5	36.5	14.2	24.6	38.8
4VP-1.0P	P(4VP-*co*-HEMA)	Pyridine	1.0	66.2	37.0	18.9	55.9
4VP-1.5P	P(4VP-*co*-HEMA)	Pyridine	1.5	73.7	48.3	17.2	65.5
4VP-0.5D	P(4VP-*co*-HEMA)	DMSO	0.5	—	—	—	38.8
4VP-1.0D	P(4VP-*co*-HEMA)	DMSO	1.0	—	—	—	55.9
4VP-1.5D	P(4VP-*co*-HEMA)	DMSO	1.5	—	—	—	65.5

[a] Molar ratio of PHPS to HEMA in feed.
[b] Molar ratio of grafted PHPS onto polymer to PHPS in feed.
[c] Weight fraction of silica in composite. Grafted: Grafted silica fraction in the composite calculated from G_{PHPS} and [PHPS]/[HEMA]. Unreacted: unreacted silica fraction in the composite calculated from G_{PHPS} and [PHPS]/[HEMA]. Overall: overall fraction of silica in the composites calculated from [PHPS]/[HEMA].

and P(4VP-*co*-HEMA). Q and e values were (Q = 0.80, e = 0.20), (1.30, −0.50) and (1.0, −0.28) for HEMA, 2VP, and 4VP, respectively. The localization of HEMA in P(2VP-*co*-HEMA) and P(4VP-*co*-HEMA) was neglected.

Grafting of PHPS on random copolymers in blend solutions

To graft PHPS onto polymer, the PHPS-xylene solution (NN-110) was blended with polymer solutions. The blend conditions are listed in Table II. The molar blend ratios of PHPS to HEMA, [PHPS]/[HEMA], varied from 0.5 to 1.5. It was previously found that when the polymer concentration of P(MMA-*co*-HEMA) was lower than 1.0 wt %, the blend solution with NN-110 did not form a gel. The polymer concentration used in of this work was 1.0 wt %. Again, no gelation was observed for all blend solutions. Taking account of the reaction time previously investigated, the maximum shelf time of the solutions before casting was set to 24 h.

PHPS grafting onto polymers and calcination of the composites was quantitatively confirmed by FTIR. Figure 2 shows FTIR spectra of P(2VP-*co*-HEMA) and its composites at [PHPS]/[HEMA] = 0.5. To confirm the grafting of PHPS onto P(2VP-*co*-HEMA), the P(2VP-*co*-HEMA) was collected from the blend solution by precipitation into cyclohexane, which is a good solvent for PHPS and a bad solvent for P(2VP-*co*-HEMA) [Fig. 2(b)]. After reaction with PHPS, new peaks assigned to Si—H and Si—N of PHPS, respectively, appeared at 2160 and 833 cm^{-1}, indicating that grafting of PHPS onto P(2VP-*co*-HEMA) had occurred. Figure 2(c) and (d) shows the FTIR spectra of the blend solution film and the calcined film, respectively. The Si—H and Si—N peaks at 2160 and 833 cm^{-1}, respectively, completely vanished after drying the blend solutions even before calcination. On the other hand, an Si—O peak appeared at 1100 cm^{-1}. The spectra of the composites did not change after calcination, indicating that calcination was complete after drying the blend solution for the composites. All PHPS in the composites was successfully converted into silica by calcination. The gradual conversion of PHPS to silica at room temperature is generally observed for the reaction of PHPS with polymer with hydroxyl groups.[19]

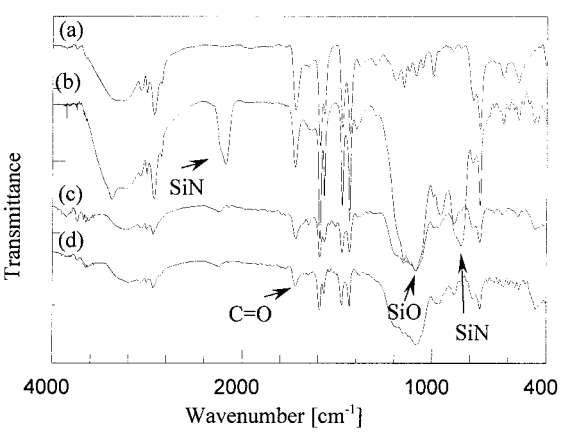

Figure 2 FTIR spectra of P(2VP-*co*-HEMA) and composites. (a) P(2VP-*co*-HEMA). (b) Purified organic polymer after blending with PHPS in pyridine at [PHPS]/[HEMA] = 0.5. (c) Dried film of blend solution of P(2VP-*co*-HEMA) and PHPS in pyridine at [PHPS]/[HEMA] = 0.5. (d) Calcined film of dried film of blend solution of P(2VP-*co*-HEMA) and PHPS in pyridine at [PHPS]/[HEMA] = 0.5.

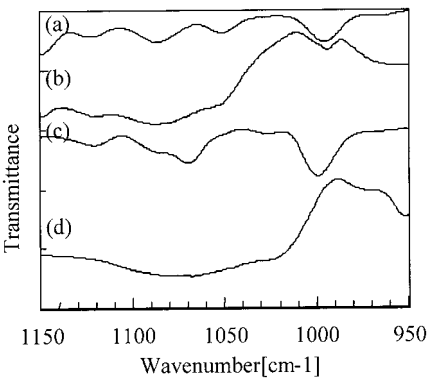

Figure 3 FTIR spectra of P(2VP-*co*-HEMA), P(4VP-*co*-HEMA), and their composites prepared in pyridine at [PHPS]/[HEMA] = 0.5. (a) P(2VP-*co*HEMA). (b) Composite of P(2VP-*co*-HEMA). (c) P(4VP-*co*-HEMA). (d) Composite of P(4VP-*co*-HEMA).

Hydrogen bond formation between 4VP and hydroxyl groups is reported in aprotic nonpolar solvents.[27,28] The aggregation of 4VP and HEMA in blend solution was investigated by FTIR in detail. Figure 3 shows the FTIR spectra of P(2VP-*co*-HEMA), P(4VP-*co*-HEMA) and the purified graft copolymers at [PHPS]/[HEMA] = 0.5. The free pyridine peak should be observed at 993 cm^{-1}. In this work, the pyridine peaks were shifted to 995 and 999 cm^{-1} for P(2VP-*co*-HEMA) and P(4VP-*co*-HEMA), respectively, due to the hydrogen bonds with HEMA. After reaction with PHPS, the pyridine peaks shifted from 995 to 993 cm^{-1} for P(2VP-*co*-HEMA), and the pyridine peak of P(4VP-*co*-HEMA) at 999 cm^{-1} vanished, indicating that the hydrogen bonding between 2VP and HEMA was broken for P(2VP-*co*-HEMA) and the novel interaction between 4VP and PHPS was formed for P(4VP-*co*-HEMA). It should be noted that the resolution FTIR of this work was 1 cm^{-1}. Thus, the shift of the peaks was not the resolution/error but the peak shift. Because there is a novel interaction between 4VP and PHPS, the enhancement of grafting of PHPS onto P(4VP-*co*-HEMA) was expected.

Conversion of PHPS, G_{PHPS} = [grafted PHPS]/[fed PHPS] (mol %), was determined for pyridine and THF solutions by using carbonyl peak at 1730 cm^{-1} and PHPS peaks at 2160 and at 1100 cm^{-1} (Si—O). G_{PHPS} could not be measured for the DMSO solutions because good precipitant was not identified. Figure 4 shows G_{PHPS} for P(2VP-*co*-HEMA) and P(4VP-*co*-HEMA) in pyridine and THF. It is quite interesting that G_{PHPS} was increased by adjusting the [PHPS]/[HEMA] molar ratio in pyridine even when the [PHPS]/[HEMA] was lower than 1.0. It was previously found that the reaction of PHPS did not quantitatively but qualitatively react with HEMA. It was due to the stereochemical shield of unreacted HEMA by PHPS grafted onto polymer chain. The shield effect more evident at higher HEMA contents. As well as before, the lower G_{PHPS} than quantitative value was due to the shield of PHPS grafted onto P(2VP-*co*-HEMA) and P(4VP-*co*-HEMA). On the other hand, G_{PHPS} was constant (ca. 100%) in THF. The hydroxyl group in HEMA was segregated in THF. THF is a good solvent for PHPS. The grafted PHPS cannot form segregation with hydroxyl group in THF. The unreacted HEMA would not be shielded by the grafted PHPS due to the strong difference of the solubility between HEMA and PHPS to THF. Therefore, from a viewpoint of G_{PHPS}, selective solvent was a better solvent to graft PHPS onto P(2VP-*co*-HEMA).

In pyridine, G_{PHPS} of P(4VP-*co*-HEMA) was higher than that of P(2VP-*co*-HEMA). The enhancement of grafting of PHPS onto P(4VP-*co*-HEMA) was due to the formation of interaction between PHPS and 4VP unit of P(4VP-*co*-HEMA) observed by FTIR.

Nanostructure of composites

The nanostructures of the composites were investigated by TEM. Figure 5 shows the transmission electron micrographs of the calcined composites of P(2VP-*co*-HEMA) prepared in THF and pyridine with [PHPS]/[HEMA] = 0.5 and 1.5. The dark regions correspond to silica domains. It was clear that the internal structure of all composites was microphase-seprarated into organic polymer and silica domains. The average sizes of the P2VP and silica domains ranged from 20 to 80 nm. Thus, P2VP/silica nanocomposites were obtained with PHPS in THF and pyridine. The clear microphase separation was observed for 2VP-0.5P with lowest G_{PHPS} in this work. It was found that enough amount of graft copolymers to form the microphase separation were formed in the composites even though the unreacted PHPS was remained in the composites. The nanostructures of composites of P(2VP-*co*-HEMA) prepared in THF [Fig. 5(a) and (b)]

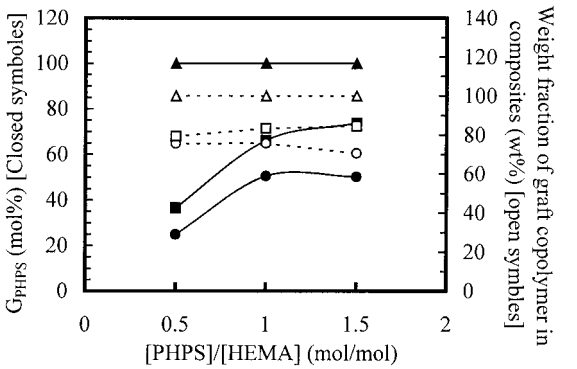

Figure 4 Effect of [PHPS]/[HEMA] on degree of grafting of PHPS onto polymer, G_{PHPS}. Circle: P(2VP-*co*-HEMA) in pyridine. Square: P(4VP-*co*-HEMA) in pyridine. Triangle: P(2VP-*co*-HEMA) in THF.

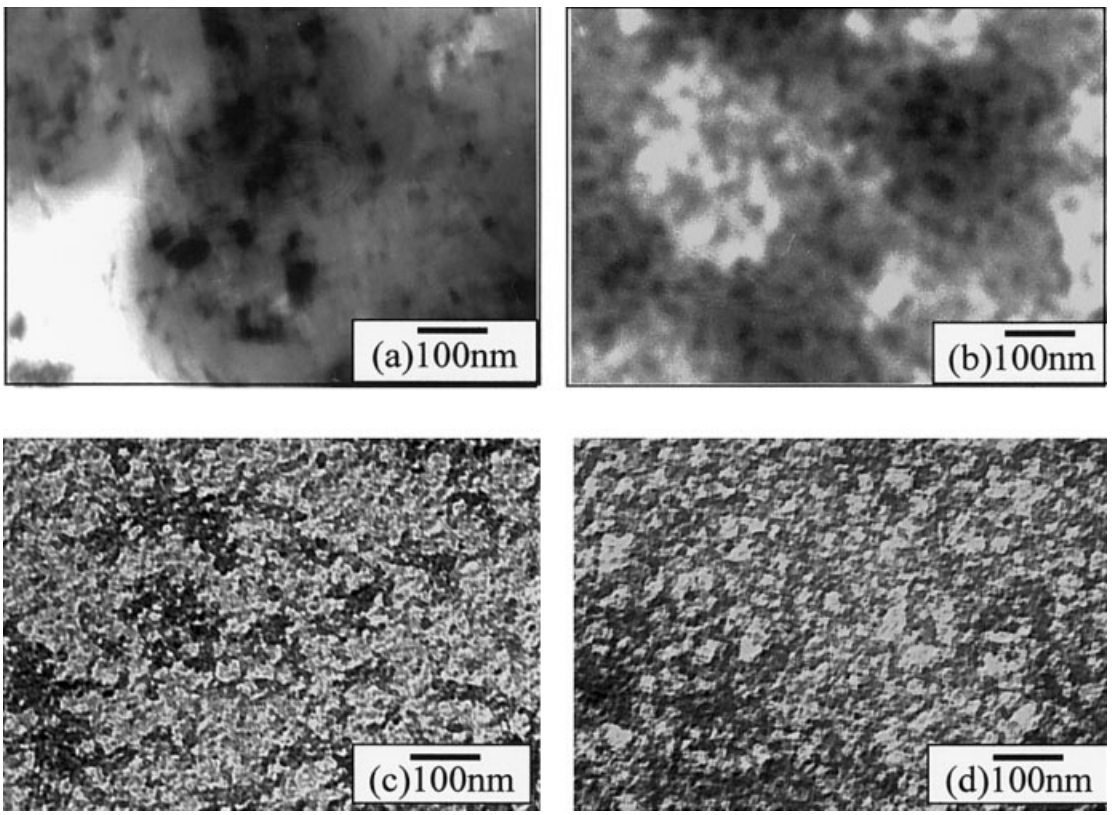

Figure 5 Transmission electron micrographs of composites of P(2VP-*co*-HEMA) (a) Prepared in THF at [PHPS]/[HEMA] = 0.5. (b) Prepared in THF at [PHPS]/[HEMA] = 1.5. (c) Prepared in pyridine at [PHPS]/[HEMA] = 0.5. (d) Prepared in pyridine at [PHPS]/[HEMA] = 1.5.

and in pyridine [Fig. 5(c) and (d)] were drastically different. When THF was used, the spherical silica domains were formed. Not the shape but the number of spherical silica domain was increased by increasing the [PHPS]/[HEMA] molar ratio. The number-average diameter, D_n, and polydispersity, D_w/D_n, were 20 nm and 1.12, respectively. The formation of spherical silica domains with relatively narrow size distributions suggests that the segregated hydroxyl groups in THF were fixed with PHPS. Thus, using a selective solvent, such as THF, improved the homogeneity of the size and the shape of the domains in the nanocomposites. However, the shape of silica domain could not be controlled by varying the [PHPS]/[HEMA] ratio. When pyridine was used, the volume fraction of continuous silica domains increased on increasing the [PHPS]/[HEMA] ratio. Generally, the shape of nanostructure of block and graft copolymers is governed by the volume fraction of each sequence, so-called Molau's law.[29] In this work, the shape of the nanostructures of the composites were dependent on the [PHPS]/[HEMA], when the composites were prepared in pyridine. Thus, the nanostructure of the composites was controlled with nonselective solvent.

Figure 6 shows the TEM micrographs of the composites of P(4VP-*co*-HEMA) prepared in pyridine and DMSO. Both pyridine and DMSO are good solvent for P(4VP-*co*-HEMA). Given the higher G_{PHPS} for P(4VP-*co*-HEMA) compared to P(2VP-*co*-HEMA), better control of the nanostructure of the composites was expected for P(4VP-*co*-HEMA) in pyridine. However, the morphologies of the nanocomposites of P(2VP-*co*-HEMA) and P(4VP-*co*-HEMA) in pyridine at the same [PHPS]/[HEMA] values were very similar. The morphologies of P4VP/silica nanocomposites prepared in pyridine and DMSO were comparable when the [PHPS]/[HEMA] were similar. Thus, nanocomposite morphology was not governed by G_{PHPS} but by the selectivity of solvent and the [PHPS]/[HEMA] molar ratio.

Thermal properties of the composites

When polymer is phase separated on a microscopic length scale, the glass transition temperature (T_g) due to each domain should be detected. Because microphase separation of silica and organic domains were observed for the composites by TEM, DSC measurements were carried out. The DSC profiles of the polymers and their composites prepared in pyridine are shown in Figure 7. The original T_g values of of P(2VP-*co*-HEMA) and P(4VP-*co*-HEMA) were 94.2 and

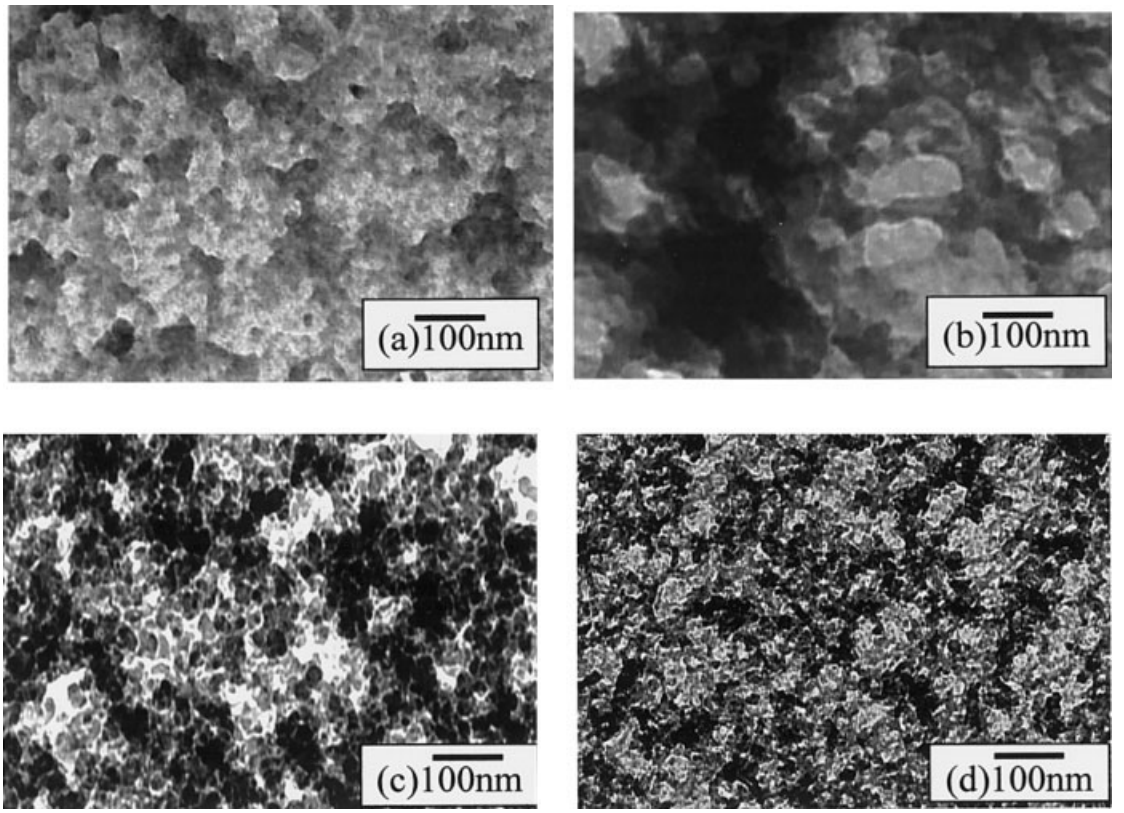

Figure 6 Transmission electron micrographs of composites of P(4VP-*co*-HEMA) (a) Prepared in pyridine at [PHPS]/[HEMA] = 0.5. (b) Prepared in pyridine at [PHPS]/[HEMA] = 1.5. (c) Prepared in DMSO at [PHPS]/[HEMA] = 0.5. (d) Prepared in DMSO at [PHPS]/[HEMA] = 1.5.

140.5°C, respectively. The T_g peak was not detected for the composites with P(2VP-*co*-HEMA). For the composites with P(4VP-*co*-HEMA), T_g seemed to be shifted to lower temperature. However, the change of the slope at ca. 90 and 125°C of 4VP-0.5P and 4VP-1.0P, respectively, were not T_g but due to the evaporation of moisture in the composites. The absent of T_g owing to the increase of compatibility between organic and silica domains has been reported in other nanocomposites.[24,30–32] Especially, when the confinement of polymer chains in domains was smaller than 15 nm, it was impossible to detect T_g by DSC.[30] The average sizes of the P2VP and P4VP domains, 20 to 80 and 10 to 50 nm, respectively, were larger than 15 nm. However, the T_g was not observed for the composites in this work. It is difficult to detect the small amount silica interpenetrated to the organic domains by TEM. The absent of T_g in this work suggests the penetration of silica into organic domains, although microphase separation was observed for the composites. The microscopic mobility of organic polymer was hindered by chemical attachment at the silica to P(2VP-*co*-HEMA) and P(4VP-*co*-HEMA).

Generally, thermal stability of organic polymer is drastically improved by the interpenetration of silica.[31] When acrylonitrile–butadiene–styrene copolymers

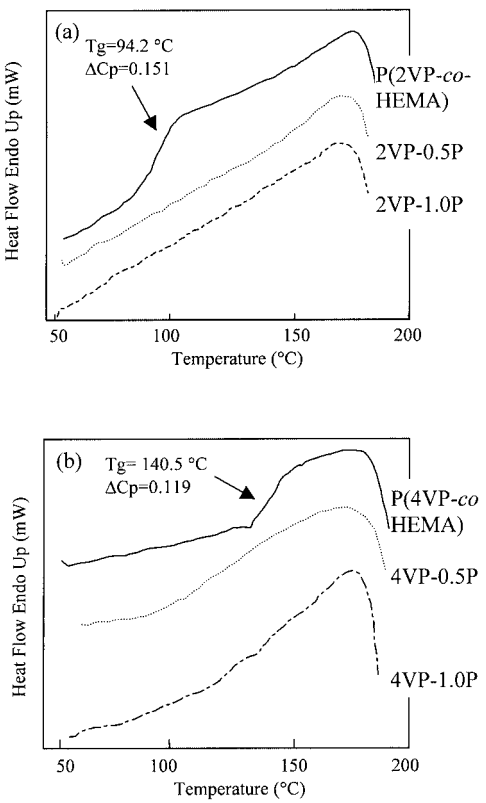

Figure 7 DSC curves of organic polymer and composites. (a) P(2VP-*co*-HEMA) and its composites. (b) P(4VP-*co*-HEMA) and its composites.

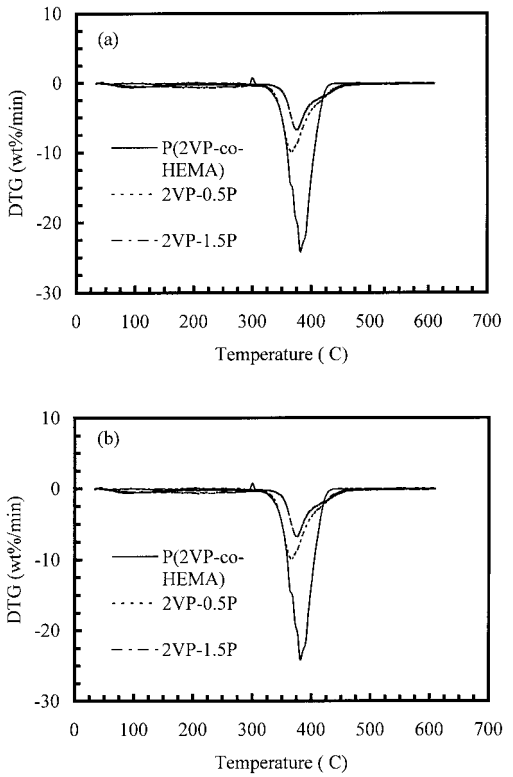

Figure 8 DTG curves of organic polymer and composites. (a) P(2VP-*co*-HEMA) and its composites. (b) P(4VP-*co*-HEMA) and its composites.

(ABS) was connected to silica domain by covalent bonds in the ABS/silica composite, the thermal stability was increased by increasing the T_g because of the increase of the compatibility between the polymer and silica phases.[32] Because T_g was not detected for the composites in this work, the improvement of the thermal stability of the composites was expected. Thus, DTG and TGA measurements were carried out, and the results are shown in Figures 8 and 9. The peak temperature of first decomposition peak and the starting temperature of decomposition, T^*, estimated from DTG measurements, and the char residue are listed in Table III. As shown in Table III, the changes of the peak temperatures of first decomposition peak between polymer and the composites were less than 14°C. Thus, the peak temperatures of first decomposition peak measured by DTG did not vary by blending with silica (Fig. 8). The composites were clearly phase separated into organic and silica domains. Thus, silica had no effect on the decomposition of organic polymer.

On the other hand, the thermal stability of the composite at low temperature was improved (TGA measurements: Fig. 9). First, T^* was drastically increased with increasing weight fraction of silica. Because T^* of P(4VP-*co*-HEMA), 281.5°C, was lower than that of P(2VP-*co*-HEMA), 323.1°C, the effect of silica on the improvement of thermal stability was clearer for P(4VP-*co*-HEMA) than P(2VP-*co*-HEMA). However, it was impossible to increase T^* over the peak temperature of first decomposition peak of P(2VP-*co*-HEMA) and P(4VP-*co*-HEMA).

As well as T^*, the char residues at 350 and 420°C were also improved for the composites. To clarify the effect of silica, the char residue corresponded to organic component, $CHAR_{polymer}$, was calculated with the weight fraction of silica and the char residue of measured by TGA. At 350°C, $CHAR_{polymer}$ of P(4VP-*co*-HEMA) was drastically increased by increasing the weight fraction of silica. The silica was not effective on $CHAR_{polymer}$ for P(2VP-*co*-HEMA) at 350°C, because T^* of P(2VP-*co*-HEMA), 323.1°C, was close to 350°C.

At 420°C, which is higher temperature than the peak tempertaure of first decomposition peak, $CHAR_{polymer}$ of all composites was in the range of 20.3–29.4 wt %, instead of 3.4 and 1.1 wt % for P(2VP-*co*-HEMA) and P(4VP-*co*-HEMA), respectively. Thus, decomposition was clearly improved at 420°C. It should be noticed that $CHAR_{polymer}$ at 420°C of the composites did not depend on the weight fraction of silica. Char residue at 600°C of all samples showed a good correlation with

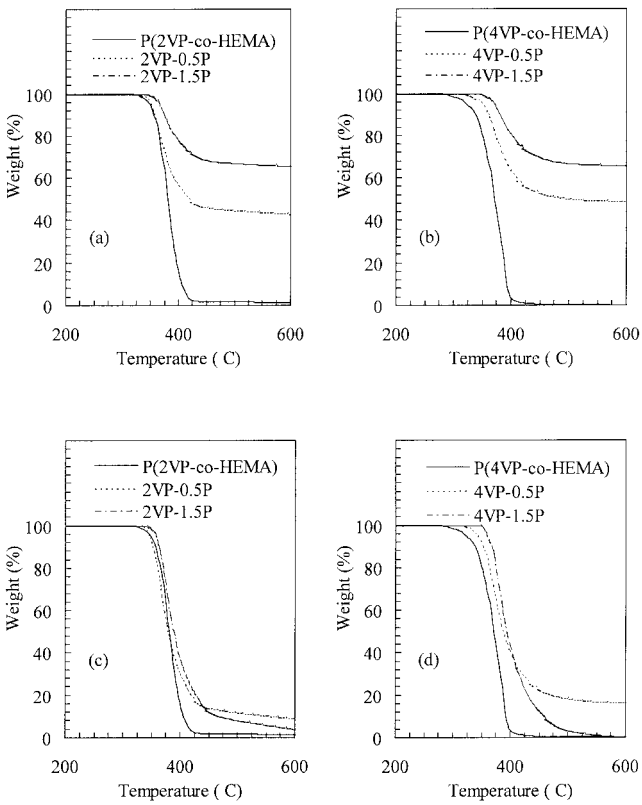

Figure 9 TGA curves of organic polymer and composites. (a) P(2VP-*co*-HEMA) and its composites. (b) P(4VP-*co*-HEMA) and its composites. (c) Corrected TGA curves to organic component of P(2VP-*co*-HEMA) and its composites. (d) Corrected TGA curves to organic component of P(2VP-*co*-HEMA) and its composites.

TABLE III
Thermal Properties of P(2VP-*co*-HEMA), P(4VP-*co*-HEMA) and Their Composites

Code	Weight fraction of silica (wt %)	T^{*a} (°C)	Char residue[b] (wt %)			$CHRA_{polymer}$[c] (wt %)			Peak temperature of first decomposition peak (°C)
			350°C	420°C	600°C	350°C	420°C	600°C	
P(2VP-*co*-HEMA)	0.0	323.1	94.0	3.4	1.3	94.0	3.4	1.3	381.2
2VP-0.5P	37.3	332.4	95.0	50.0	42.9	92.0	20.3	8.9	367.4
2VP-1.5P	64.1	346.0	99.2	72.7	65.5	97.8	23.9	4.1	377.4
P(4VP-*co*-HEMA)	0.0	281.5	78.4	1.1	0.2	78.4	1.1	0.2	383.7
4VP-0.5P	38.8	327.8	93.6	56.8	48.8	89.6	29.4	16.3	374.9
4VP-1.5P	65.5	350.5	99.4	74.0	65.6	98.3	24.6	0.2	384.4

[a] Starting temperature of decomposition.
[b] Char residue of the composite.
[c] Char residue corresponding to organic component calculated from the weight fraction of silica in the composites.

the weight fraction of silica of samples, indicating that the organic component was completely decomposed at 600°C for any samples. Consequently, thermal properties lower than 420°C were clearly improved for the organic/silica composites of both P(2VP-*co*-HEMA) and P(4VP-*co*-HEMA).

CONCLUSION

Organic polymer and silica nanocomposites were synthesized with perhydropolysilazane [PHPS] and poly(2-vinyl pyridine-*co*-2-hydroxyethyl methacrylate) [P(2VP-*co*-HEMA)] or poly(4-vinyl pyridine-*co*-2-hydroxyethyl methacrylate) [P(4VP-*co*-HEMA)] in pyridine, THF, and DMSO. When polymer and PHPS were blended in nonselective solvent such as pyridine and DMSO, the nanostructures of the composites did not depend on the selectivity of the solvent but instead on the feed ratio of PHPS to HEMA. When a selective solvent such as THF was used, the nanostructure of the composites was spherical silica with narrow size distribution, where size was independent of the blend ratio. It was due to the aggregation of hydroxyl groups in THF. The degree of grafting of PHPS on P(4VP-*co*-HEMA) was enhanced, because of the interaction between P4VP and PHPS in pyridine. The T_g of organic domain of the composites vanished, T^* increased, and the thermal stability was improved over the range of 350–420°C.

The authors would like to acknowledge Clariant Japan Co. for providing us with NN-110.

References

1. Judeinstein, P.; Sanchez, C. J Mater Chem 1996, 6, 511.
2. Novak, B. M. Adv Mater 1993, 5, 422.
3. Ravaine, D.; Seminel, A.; Charbouillot, Y.; Vincens, M. J Non-Cryst Solid 1986, 82, 210.
4. Judeinstein, P.; Titman, J.; Stamm, M.; Schmid, H. Chem Mater 1994, 6, 127.
5. Brik, M. E.; Titman, J. J.; Bayle, J. P.; Judeinstein, P. J Polym Sci Part B Polym Phys 1996, 34, 2533.
6. Shimid, H.; Poppal, M.; Rousseau, F.; Poinsignon, C.; Armad, M.; Rousseau, J. Y. 2nd Int. Sym. Polym. Elecrtolytes, 1989, p. 325.
7. Chujo, Y. Curr Opin Solid State Mater Eng 1996, 1, 806.
8. Brink, C. J.; Scherer, G. W. Sol-Gel Science: The Physics and Chemistry of Sol-Gel Processing; Academic Press: San Diego, 1990.
9. Schmid, H. J Non-Cryst Solids 1985, 73, 681.
10. Wen, J.; Wilkes, G. L. Chem Mater 1996, 8, 1667.
11. Schmid, H.; Wolter, H. J Non-Cryst Solids 1990, 121, 428.
12. Saegusa, T.; Chujo, Y. J Macromol Sci Chem 1990, A27, 1603.
13. Chujo, Y.; Ihara, E.; Kure, S.; Suzuki, K.; Saegusa, T. Makromol Chem Macromol Symp 1991, 42/43, 303.
14. Molau, G. E., Ed. In Colloid and Morphological Behaviour of Block Copolymers; Plenum Press: New York, 1971.
15. Meier, D. J. Block Copolymers; Science and Technology; Gordon and Breach Science Publisher: Tokyo, 1983.
16. Pyun, J.; Matyjaszewski, K. Macromolecules 2000, 33, 217.
17. Kim, B.-S.; Mather, P. T. Macromolecules 2002, 35, 8378.
18. Saito, R.; Kuwano, K.; Tobe, T. J Macromol Sci Pure Appl Chem 2002, A39, 171.
19. Saito, R.; Mori, Y. J Macromol Sci Pure Appl Chem 2002, A39, 915.
20. Mori, Y.; Saito, R. J Macromol Sci Pure Appl Chem 2003, A40, 671.
21. Sarma, N. S.; Dass, N. N. Mater Sci Eng B Solid-State Mater Adv Technol 2001, 79, 78.
22. Nugay, N.; Kucukyavuz, Z.; Kucukyavuz, S. Polymer 1993, 34, 4649.
23. Percy, M. J.; Barthet, C.; Lobb, J. C.; Khan, M. A.; Lascelles, S. F.; Vamvakaki, M.; Armes, S. P. Langmuir 2000, 16, 6913.
24. Amalvy, J. I.; Percy, M. J.; Armes, S. P. Langmuir 2001, 17, 4770.
25. Biggs, S.; Proud, A. D. Langmuir 1997, 13, 7202.
26. Arichi, S. Bull Chem Soc Jpn 1966, 39, 439.
27. Ruokolainen, J.; ten Brinke, G.; Ikkala, O.; Tokkeli, M.; Serimaa, R. Macromolecules 1996, 29, 3409.
28. Ruokolainen, J.; Saariaho, M.; Ikkala, O.; ten Brinke, G.; Thomas, E. L. Macromolecules 1999, 32, 1152.
29. Molau, G. E. Colloidal and Morphological Behaviour of Block Copolymers; Plenum Press: New York, 1971.
30. Motomatsu, K.; Takahashi, T.; Nie, H.-Y.; Mizutani, W.; Tokumoto, H. Polymer 1997, 38, 177.
31. Hajji, P.; David, L.; Gerard, J. F.; Pascault, J. P.; Vigier, G. J Polym Sci Part B Polym Phys 1999, 37, 3172.
32. Hsu, Y. G.; Lin, F. J. J Appl Polym Sci 2000, 75, 275.